Evaluation methods for the scaling power of water

METHODES D'EVALUATION DU POUVOIR ENTARTRANT DE L'EAU

F. HUI, J. LÉDION

LM3, CNRS UPRESA 8006, ENSAM, 151, Boulevard de l'Hôpital, 75013 Paris - France

Résumé

Durant ces 20 dernières années diverses méthodes d'étude de l'entartrage se sont développées. Dans cet exposé on passe en revue toutes les méthodes qui présentent un intérêt pratique et qui reposent sur des bases scientifiques sérieuses. Ainsi la majorité des techniques d'évaluation de l'entartrage sont présentées dans cette mise au point. Ces méthodes peuvent être classées en deux grandes catégories : les méthodes électrochimiques et les méthodes non électrochimiques. La première catégorie est constituée de la chronoampérométrie, de la chronoélectrogravimétrie et de l'impédancemétrie électrochimique qui sont toutes fondées sur le principe de la réduction de l'oxygène dissous dans l'eau par la polarisation d'une électrode métallique à un potentiel suffisamment négatif.

Parmi les méthodes non électrochimiques, nous pouvons citer la méthode du pH critique, deux méthodes thermiques, une méthode à évaporation, la méthode LCGE, la méthode de précipitation contrôlée rapide, une méthode d'entartrage sur polymères et une méthode sur tubes en continu.

Toutes ces méthodes présentent des avantages et des inconvénients, mais leur complémentarité est souvent utile lorsqu'on veut traiter un problème concret d'entartrage. Cependant les techniques les plus récentes ont été développées pour tenir compte, et si

possible éviter, la plupart des inconvénients des méthodes antérieures. On peut donc affirmer que les méthodes d'entartrage sur polymère, sur tubes en continu ainsi que la méthode de Précipitation Contrôlée Rapide permettent de travailler dans des conditions thermodynamiques tout à fait réalistes car elles permettent d'entartrer avec un facteur de sursaturation nettement inférieure à 40. On se place bien ainsi dans le domaine de l'entartrage et non pas dans le domaine de la précipita tion spontanée homogène. L'étude des divers traitements antitartre proposés devient tout à fait possible et de manière très pertinente.

Abstract

Various methods on scaling study have been developed during the last 20 years. In this article, we review all methods, based on reliable scientific principles, which show a practical interest. These methods can be roughly divided into two categories: electrochemical methods and non-electrochemical methods. The first one is made up of chronoamperometry, chronoelectrogravimetry and electrochemical impedance technique which are all based on the reduction of the oxygen dissolved in the test water by polarizing a metallic electrode at a sufficiently negative potential.

Among the non-electrochemical methods, we can enumerate the critical pH method, two thermal methods, an evaporation method, the LCGE method, the rapid controlled precipitation method, a polymer scaling test and a continuous test on tubes.

All these methods have advantages and drawbacks, but their complementarity is often useful when we are confronted with the treatment of a real scaling problem. Nevertheless, the newest techniques have been developed in taking into consideration their representetiveness in relation to a real-life scaling phenomenon, and if possible, to avoid major drawbacks of the previous methods. Hence, we can state that the methods such as the tests on polymers and on tubes as well as the Rapid Controlled Precipitation (RCP) allow to establish thermodynamic conditions where the scaling is formed with a degree of oversaturation much less than 40. In other words, the experimental conditions of these three methods lead to a real scaling but no a spontaneous and homogenous precipitation of $CaCO_3$. Thus, the study of various proposed antiscaling treatments becomes entirely possible.

Key words : *water, scaling, calcium carbonate, scaling evaluation, antiscaling treatment*

INTRODUCTION

Scaling in natural hard water is a major concern in different facets of industrial processes and domestic installations (Legrand & Leroy, 1990; Roques, 1990). Undesirable scale deposits often cause numerous technical and economical problems such as total or partial obstruction of pipes leading to a decrease in flow rate; reduced heat transfer as calcium carbonate precipitate is 15 to 30 times less conductive than steel; seizure of valves and clogging of filters, etc. In nuclear power plants, the power produced is often limited by scaling in cooling towers. In Great Britain, the non-productive expenses related to scaling were estimated at 600 million pounds per year (Gabielli et al., 1997). The same expenses are about 1.5 billion euros per year in France (Rosset, 1992). Hence, it is of vital importance to establish appropriate methods to study this phenomenon and to find effective ways to prevent or combat it.

For decades, various attempts (Gabielli et al., 1997; Lédion et al., 1985; Lin et al., 1990; Feitler, 1972; Leroy et al., 1993; Khalil et al., 1992; Lin et al., 1995; Dufeau et al., 1995; Rosset at al., 1996; Gabrielli et al., 1996; Rosset et al., 1997; Euvrard et al., 1997; Hort, 1994; Elfil & Roques, 2001) have been made to estimate the scaling power of natural waters and characterise the scaling formation mechanisms. We describe herein major different methods developed to date by emphasising whether they are representative with respect to a real-life scaling formation process.

ELECTROCHEMICAL METHODS

The first electrochemical method, chronoamperometry, has been proposed by Lédion (Lédion et al., 1985). It is based on the electrochemical reduction of the oxygen dissolved in the test water by polarising a metallic electrode at a potential sufficiently negative according to:

$$O_2 \ + \ H_2O \ + \ 4e \ \hat{U} \ 4OH^-$$
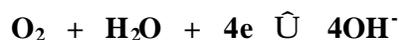
The generation of hydroxide ions in the vic inity of the electrode can increase the local pH for several pH units (Gabielli et al., 1996) and forces calcium carbonate to precipitate in a solid crystalline phase through two steps:

$$HCO_3^- \; + \; OH^- \; \Leftrightarrow \; CO_3^{2-} \; + \; H_2O$$

$$Ca^{2+} \; + CO_3^{2-} \; \Rightarrow CaCO_3(s)$$
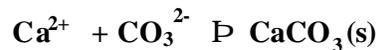
The limiting current intensity I_L, which is proportional to the flow of oxygen moving by convective diffusion towards the electrode, decreases whereas the active surface is progressively blocked by the growth of scale. Finally, I_L reaches a value close to zero when the surface is totally covered by the $CaCO_3$ insulating layer.

The $CaCO_3$ masse and the electrochemical impedance can also be measured with respect to time during scaling while the electrode was polarised at the limiting current for oxygen reduction. They are called the chronoelectrogravimetry and the electrochemical impedance technique respectively.

Chronoamperometry

A typical chronoamperometric curve is shown in Figure 1. It is characterised by a falling current shape with time whose slope is related to the scaling rate (Lédion et al., 1985; Lin et al., 1990). Lédion defined the scaling time, t_s, as the intersection of the tangent at the inflexion point of this curve and the time axis. It gives a rough estimate of the scaling potentiality of waters. The residual current i_{res} is somewhat related to the deposit morphology: the more compact and insulating the scale, the lower the residual current.

Figure 2 gives an example of application of the chronoamperometry that illustrates the efficiency of a physical antiscale treatment.

It is noted that when the electrode surface is partially blocked, the observed current due to the diffusion-limited oxygen reduction largely underestimates the actual scale coverage (Deslouis et al., 1997).
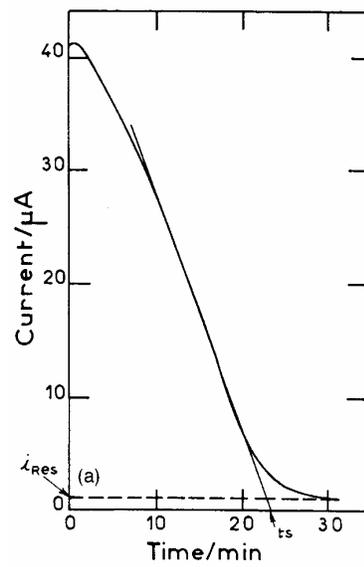
Fig. 1. A typical chronoamperometric curve. t_s : scaling time; i_{res} : residual current [Gabielli et al., 1996a].

Courbe type de chronoampérométrie. t_s : temps d'entartrage ; i_{res} : courant résiduel
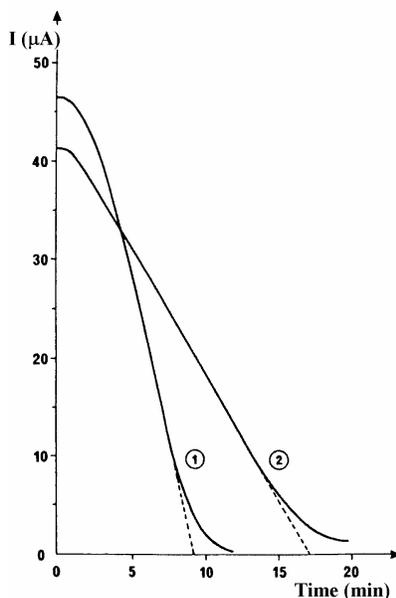
Fig. 2. Chronoamperometic curves of a raw water (1) and the same water treated by a microelectrolyse process (2) [Rosset, 1993].

Courbes chronoampérométriques d'une eau brute (1) et de la même eau traitée par un procédé de microélectrolyse.

Chronoelectrogravimetry

This method is the combination of the chronoamperometry and a quartz microbalance by which it is now possible to continuously follow extremely tiny mass changes (Khalil et al., 1992). An experimental set-up is shown in Figure 3. The working electrode is a gold disc which, in fact, is one of the two excitation electrodes of quartz crystal resonator inserted in an electronic oscillator. The frequency change, Δf, is proportional to the masse of scale deposited, Δm, on the electrode surface according to:

$$\Delta f = -2f_o^2 \Delta m/dvS$$

where f_o is the quartz resonance frequency, d, the quartz density, v, the speed of ultrasonic wave in the quartz and S, the active surface of the quartz.

Figure 4 shows a chronoelectrogravimetry curve which exhibits three steps in the scaling process: (1) during the first 10 to 25 min (see insert) the mass of scaling increases slowly; (2) from 20 to 150 min the mass of scaling increases proportionally with time (i.e., with a constant rate); (3) beyond 150 min the mass of scaling increases very slowly and this

region is called "plateau" even though the mass is still generally increasing slightly. From this curve, several characteristic parameters can be defined:

- t_N, the nucleation time corresponding to the end of the first stage. This is defined by the intersection of the linear part and the time axis;

- V_S, the scaling rate which is the slope of the intermediate linear part;

- t_S, the scaling time corresponding to the end of the intermediate stage. It is defined by the intersection of the linear part and the plateau;

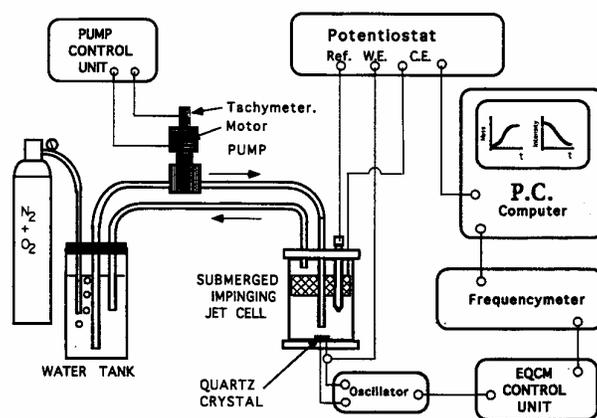Figure 5 shows the effect of a scale inhibitor ATMP by chronoelectrogravimetry.

Fig. 3. Scheme of the experimental set-up, including the submerged impinging jet cell, the water supply system, the quartz crystal microbalance with its frequency meter, the electrochemical control and the monitoring by a PC computer [Gabrielli et al., 1999]

Shéma d'un montage expérimental de la chronoélectrogravimétrie. Les éléments constitutifs essentiels sont: la cellule à jet immergé, le dispositif de préparation de l'eau synthétique, la microbalance à quartz avec un fréquencemètre, l' ordinateur qui assure le contrôle électrochimique et le traitement des donnés.
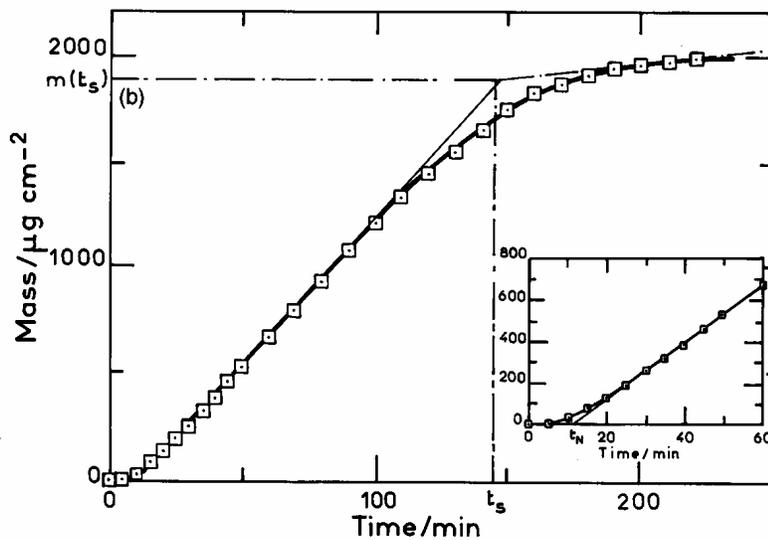
Fig. 4. Chronoelectrogravimetric curve (variation of CaCO₃weight against time) for a natural water. t_N: nucleation time, t_s: scaling time [Gabrielli et al., 1996a].

Courbe chronoélectrogravimétrique (variation de la masse de CaCO₃ en fonction du temps) d'une eau naturelle. t_N: temps de germination, t_s: temps d'entartrage.
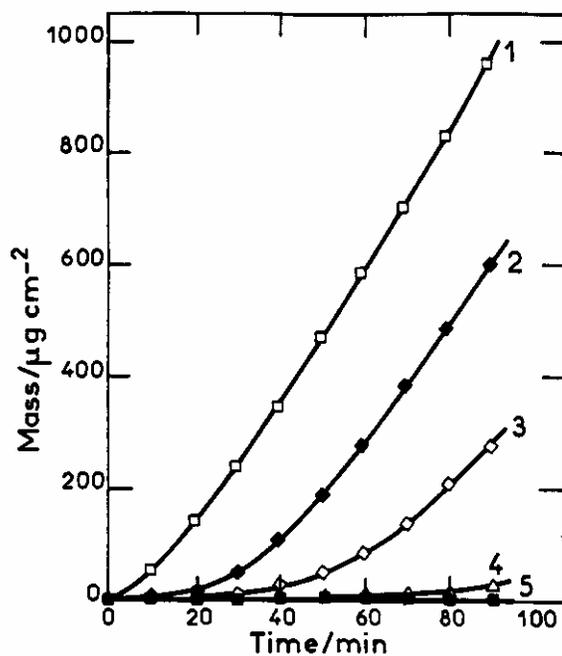

Fig. 5. Chronoelectrogravimetric curves plotted for various ATMP concentrations. (1) no addition; (2) 0.25; (3) 0.3; (4) 0.35 and (5) 0.6 mg/L [Gabrielli et al., 1996a].

Courbes Chronoélectrogravimétriques obtenues pour une eau additionnée de ATMP à des concentrations différentes.

Electrochemical impedance technique

The theory of this method has been described in details in several papers (Gabielli et al., 1997; Deslouis et al., 1997). During the scaling process, the measurement of the electrochemical impedance shows two time constants more or less well separated. It is demonstrated that the high frequency time constant allows a pseudo high frequency resistance R_{HF} and a pseudo high frequency capacitance C_{HF} which are related to the coverage of the scale (Gabielli et al., 1996). Generally, the higher the R_{HF} value, the more compact and more adherent the scale deposit. The low frequency time constant is related to the oxygen diffusion in the bulk solution.

An impedance diagram is given in Figure 6 where the high frequency resistance R_{HF} and the pseudo characteristic frequency f_{HF} are indicated. C_{HF} can be obtained from these values through $2\pi f_{HF} R_{HF} C_{HF} = 1$. A fitting procedure to a model, based on a simplex algorithm, can be used to estimate R_{HF} and f_{HF}.
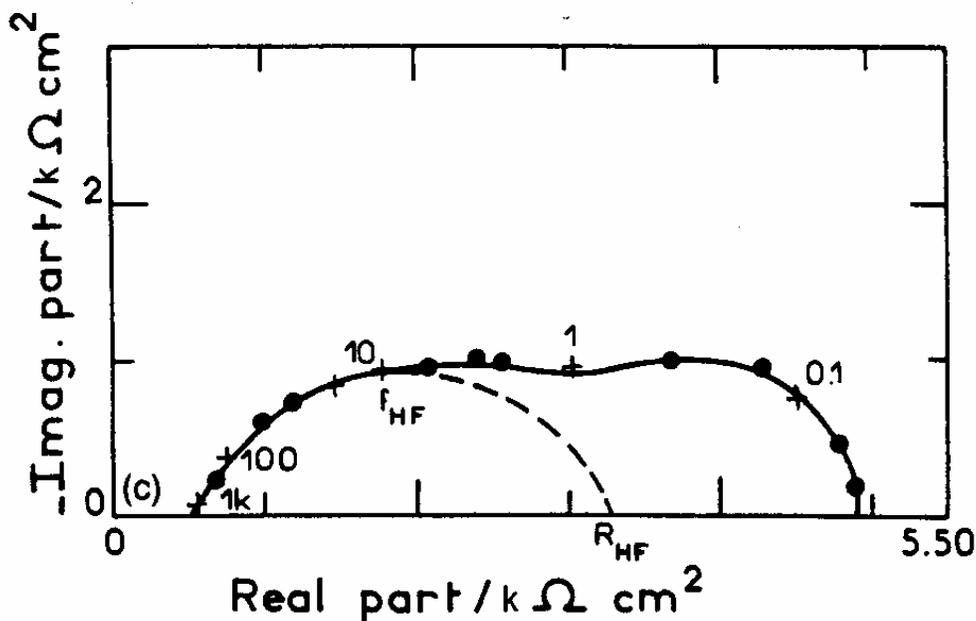
Fig. 6. Electrochemical impedance diagram. R_{HF}: pseudo high frequency resistance; C_{HF}: pseudo high frequency capacitance [Gabrielli et al., 1996a].

Diagramme d'impédance électrochimique. R_{HF} : pseudo résistance haute fréquence ; C_{HF} : pseudo capacitance haute fréquence.

The impedance diagram in Figure 7 confirm the effect of the scale inhibitor ATMP shown in Figure 5 by chronoelectrogravimetry.

It is noted that even though the use of impedance technique can considerably improves the understanding of the electrochemical scaling process, this approach is much too complicated and time consuming to be used in practical situations (Gabrielli et al., 1998).

Based on the electrochemical production of OH^- ions, Lin et al. have also developed an automatic scaling detector which has been used in a nuclear power plant (Lin et al., 1995).
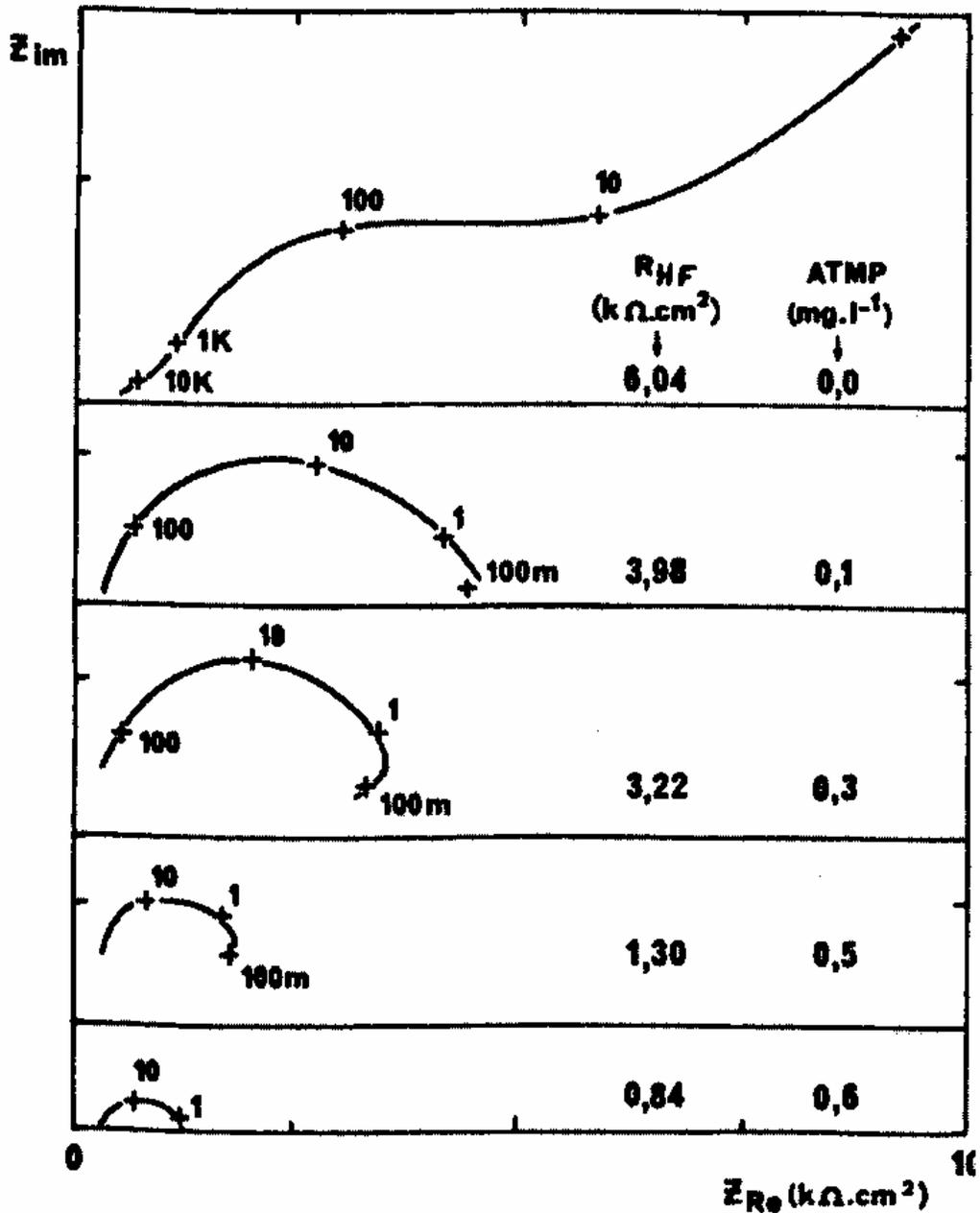
Fig. 7. Impedance diagrams of CaCO $_3$ deposits obtained from the tap water of Paris and the same water additioned with ATMP of growing concentration [Rosset, 1993].

Diagrammes d'impédance de dépôts de CaCO$_3$ obtenus à partir de l'eau de Paris et de la même eau additionnée d'ATMP en concentration croissante.

NON-ELECTROCHEMICAL METHODS

Critical pH method

The critical pH method, proposed by Feitler (Feitler, 1972) is based on the fact that there is a critical pH above which scaling occurs. That is, when the actual pH exceeds the critical pH, precipitate forms in the bulk solution, and the pH undergoes a self-reduction. In fact, the following pertinent reactions are involved in the scaling formation:

$$OH^- + H^+ \Leftrightarrow H_2O \qquad (1)$$

$$H_2CO_3 \Leftrightarrow H^+ + HCO_3^- \qquad (2)$$

$$HCO_3^- \Leftrightarrow H^+ + CO_3^{2-} \qquad (3)$$

$$CO_3^{2-} + Ca^{2+} \Rightarrow CaCO_3 \qquad (4)$$

As NaOH is added to the water, OH^- neutralises H^+ in reaction (1). This removes H^+ from reactions (2) and (3) which causes these reactions to shift to the right, generating more free CO_3^{2-} in solution. As more NaOH is added, this process continues with accompanying pH increase until enough free CO_3^{2-} is present to exceed the solubility of $CaCO_3$ and its precipitation occurs. Reaction (4) shows that as $CaCO_3$ is formed, free CO_3^{2-} is removed from solution, this upsets the equilibrium of reaction (3). To restore the needed balance, reaction shifts to the right to generate more free CO_3^{2-} and, at the same time, creates additional H^+. The presence of additional H^+ lowers the pH. It is this sequence which causes the pH to decrease as additional NaOH is added.

The critical pH (pHc) is determined by adding to water an increment of NaOH and plotting the resultant pH. A plot of typical data is shown in Figure 8. The point on the extension of the curve just above the first downturn (the maximum) of the curve is pHc.

Figure 9 gives an example of application of this method for the effect of a scale inhibitor.
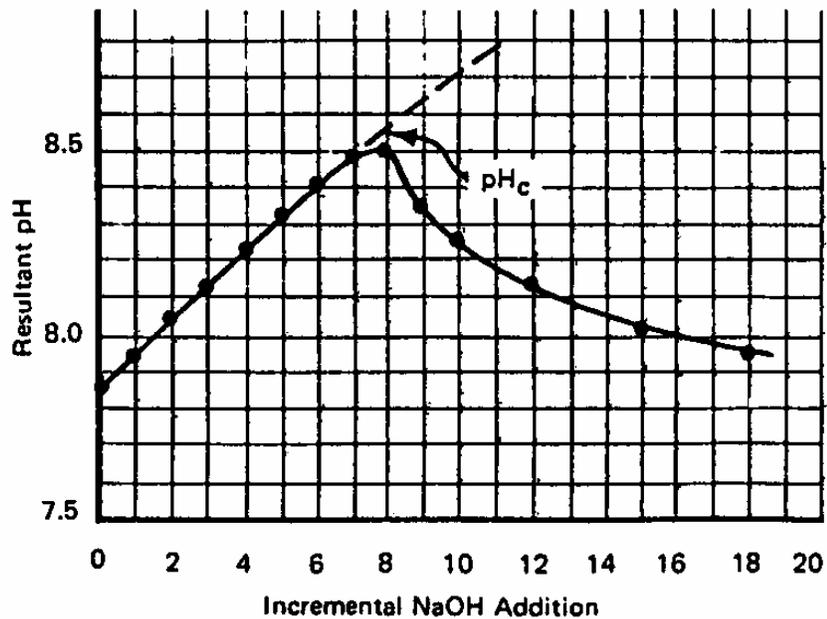
Fig. 8. Addition of NaOH and plotting the resultant pH [Feitler, 1972].

Méthode du pH critique: variation du pH en fonction de l'addition de NaOH.
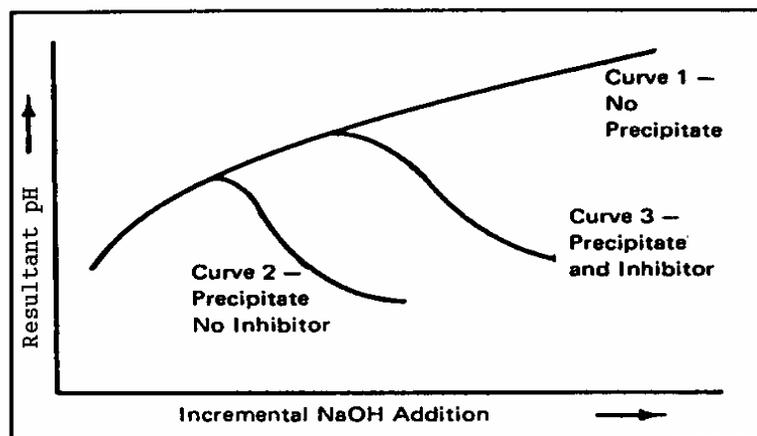

Fig. 9. Incremental addition of NaOH versus the resultant pH [Feitler, 1972].

Méthode du pH critique: effet de l'ajout d'un inhibiteur d'entartrage sur la courbe de pH en fonction de l'addition de NaOH.

Thermal methods

In real-life situations, scale deposits are formed mainly through thermal effects. In fact, heating of the water has the consequence that carbon dioxide solubility decreases, pH increases and finally calcium carbonate precipitates.

Duffau has developed a scale detector, commercialised under the trademark of Scalmatic (Duffau et al., 1995), which is based on the temperature measurement of the wall of a tube in which the test water flows through. The tube is heated by an electric resistance surrounded externally. When scale deposits form on the tube wall, the heat transfer towards the water slows down and this leads to an increase of temperature on the tube wall. The temperature variation is determined by incorporated thermocouples with a sensibility of 0.2 °C. The major drawback of this device is the use of great volume of water which circulates across the tube.

Rosset et al. have proposed an other thermal method by using a thermal sensor and the electrochemical impedance technique (Rosset et al., 1996; Gabrielli et al., 1996). The experimental set-up is the same than that in Figure 3 except that the disc electrode (thermal sensor), made of iron, is inserted through the bottom of the submerged impinging jet (SIJ) cell and a miniaturised temperature probe is located very close to the electrode active surface. The temperature of the electrode is controlled by an electronically regulated electric heater. The tank of carbonically pure water (i.e. water containing only calcium and carbonate ions) is thermostated to maintain the temperature of the solution bulk at 25 °C. By using this flow cell, the temperature of the bulk solution is not influenced significantly by the electric heater. Thus this device prevents scale deposition in the whole cell. The whole electrolyte loop is closed and maintains at equilibrium with the atmospheric pressure. The electrode is polarised by using a galvanostat at a zero d.c. current. Impedance measurements are performed by means of a frequency response analyser (Gabrielli et al., 1996).

An example of the application of this method is shown in Figure 10 (Rosset et al., 1997). The high frequency resistance R_{HF}, which is a measurement of the coverage of the electrode (thermal sensor), increases with time. It is clearly that the thermal sensor is blocked

more quickly with a harder water (Contrexéville, 117°F) than an other water (synthetic water, 50 °F). The addition of an organic phosphonate (ATMP) at a concentration of 1 mg.L^{-1} in Contrexéville water inhibits practically the formation of scale deposits. The efficiency of this scale inhibitor is thus confirmed.
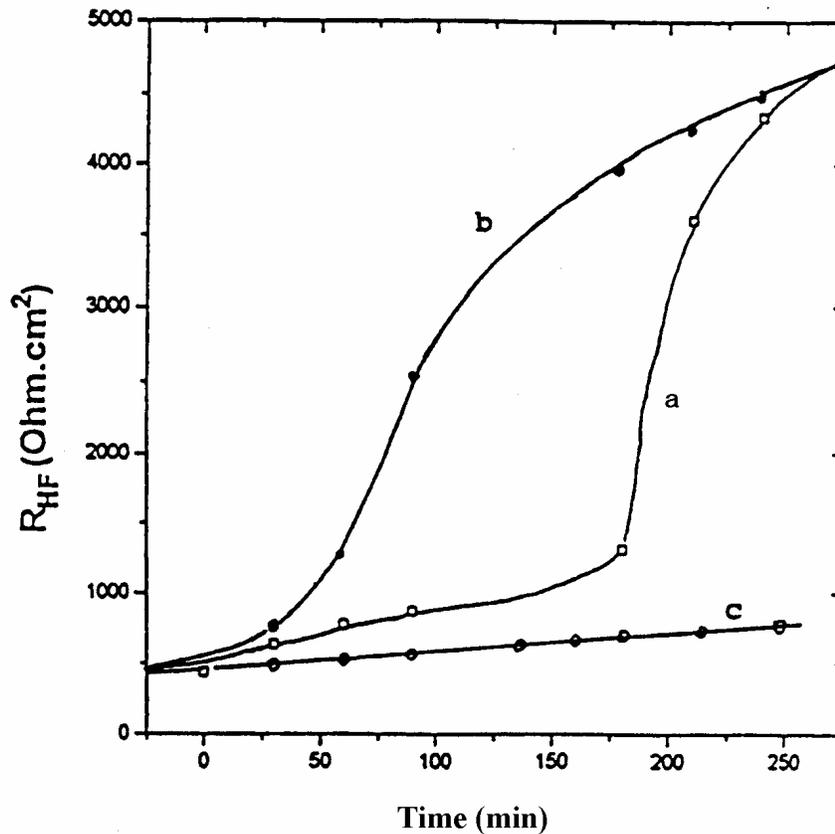
Fig. 10. Variation of the high frenquency resistance versus heating time.
a: carbonically pure water of 50 °F;
b: Contrexéville mineral water (117 °F);
c: Contrexéville mineral water added of 1 mg/L of ATMP [Rosset et al., 1997].

Variation de la résistance haute fréquence en fonction du temps de chauffage.
a : eau carboniquement pure de 50 °F ;
b : eau minérale de Contrexéville (117 °F) ;
c : eau minérale de Contrexéville additionnée de 1 mg/L d'ATMP.

Evaporation Method

This test is based on the evaluation of the number of crystals, N, present in samples of supersaturated water (Euvrard et al., 1997). As shown in Figure 11, after concentration in a rotary evaporator with a vacuum pressure of 25 mbar, water is collected in a closed glass beaker and placed in an oven at a temperature of 20 °C for a period of 24 h. Then it is filtered and two different types of analyses are consecutively carried out:

- a chemical analysis to determine the precipitated mass of $CaCO_3$;
- a morphometric analysis to define the mean characteristics of the crystals (diameter, shape and length).

As the precipitated mass of $CaCO_3$ and the mean particle size are known, it is possible to calculate the number of crystals, N, present in sample brought to a unit quantity of Ca^{2+} present before concentration:

$$N = M/(4\Pi r^3 \rho Qa/3)$$

Where N is the number of crystals present per mole of Ca^{2+}, M is the precipitated mass (g), Qa is the quantity of $CaCO_3$ contained in the sample before concentration, r is the mean particle radius (cm) and ρ is the volumic mass of crystalline variety present in the sample (g/cm^3).

When the treated and untreated water samples are compared, the test indicates whether or not the device has brought about a modification in the crystallogenesis of $CaCO_3$. Quantitatively, the effect of the device is determined as follows:

$$E = [(N_t/N_n) - 1] \times 100$$

where N_t is the number of crystals present in a sample of treated water and N_n is the number of crystals present in a sample of untreated water. The device has a positive effect if it increases the formation of crystals in the liquid, i.e. if N_t is larger than N_n.

```
Concentrated        Waiting time     Filtration and        Image
water (2X)          ─────────→       drying of        analysis of       ─────→    size
                    24 hr            the precipitate    crystals
    │                                    │                 │                         │
    ↓                                    ↓                 ↓                         ↓
initial [Ca²⁺]         and          final [Ca²⁺]  ──→   % precipitation  ──→    number N
                                                                                  of crystals
```
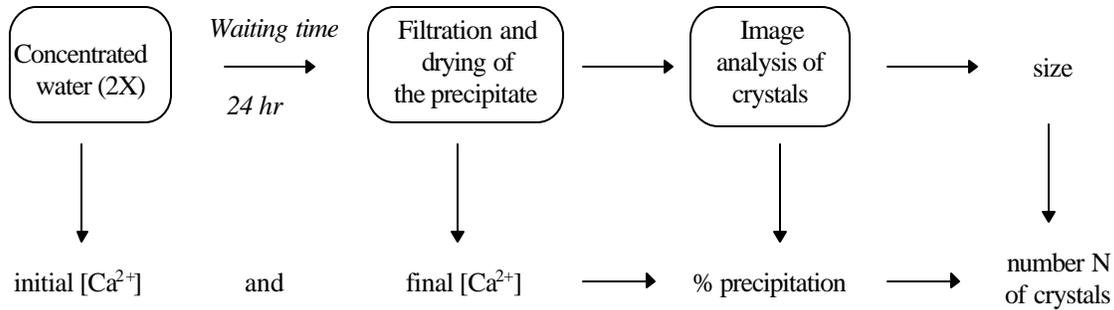
Figure 11 : Test of scaling potentiality using Evaporation method.[Euvrard et al., 1997]

Test de la potentialité d'entartrage par la méthode par évaporation.

Methods related to CO_2 degassing

LCGE method

This method, proposed by Roques et al. (Hort, 1994; Elfil & Roques, 2001), aims at the dissociation of the different kinetic stages to isolate the most limiting one that is often the mass transfer on the solid-liquid interface. The experimental installation is shown in Figure 12. Firstly, a pure calco-carbonic water is prepared by the stripping of CO_2 in an aqueous suspension of $CaCO_3$ according to:

$$CO_2 \; + \; H_2O \; + \; CaCO_3 \; \rightleftharpoons \; Ca \; + \; 2HCO_3$$

After the complete dissolution of $CaCO_3$, the stripping gas CO_2 is replaced by a mixture CO_2-air in which the CO_2 partial pressure is lower than the equilibrated CO_2 pressure (pCO_2) of the calco-carbonic solution. In this way, the supersaturation is created and this leads finally to nucleation and precipitation of $CaCO_3$. The amplitude of the supersaturation can be adjusted according to the initial concentration of the solution, the pCO_2 of the stripping gas and the temperature. As illustrated in Figure 12, the evolution of pH and [Ca] is followed along the experiment. The pCO_2, the ionic activity product and the supersaturation of the solution can

be determined by a calculation code. The deposited crystals can be collected on a trap and identified by a scanning electronic microscopy (SEB). The quartz crystal microbalance allows following the reaction on the solid sensor immersed in water.
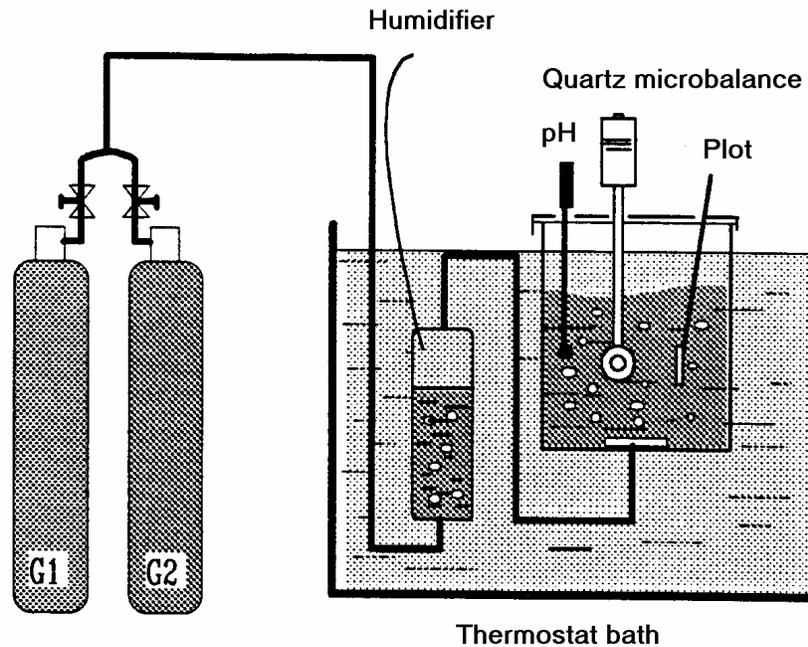

Fig. 12. Experimental set-up of the LCGE method [Hort, 1994].

Montage expérimental de la méthode LCGE.

Rapid controlled precipitation method

This method is proposed by Lédion et al. (Lédion et al., 1998) which consists in degassing of CO_2 from the test water by a moderated agitation using a magnetic stirrer. In this way, the nucleation and the growth of $CaCO_3$ are initiated in a similar way of a natural scaling phenomenon. The water scaling capacity is then characterised by taking measurements of pH and resistivity as a function of time. An experimental set-up is presented in Figure 13. In order to take into account inevitable variations in the scaling potential of the supplied water , the room temperature and the partial pressure of CO_2 during the test, parallel tests are always

performed on samples taken at the same time. The test water (treated water) and the reference water (untreated water) are stirred simultaneously in sequence of 5 or 10 minutes. After each sequence, the pH and the resistivity of the two waters are measured. Figure 14 shows an example of the variation of the pH and resistivity with time for a non-treated reference water and the same water treated by a physical antiscaling procedure. The maximum in the pH-time curves corresponds to the precipitation threshold in the water concerned. The start of precipitation is also indicated by a change in slope of the resistivity-time curves, while the slope beyond the inflection characterises the kinetics of the $CaCO_3$ precipitation.

This method is very sensitive. It has been used to assess the efficiency of a magnetic treatment of water and the residual effect of an electric treatment after 10 week's storage of the treated water (Lédion et al., 1998).
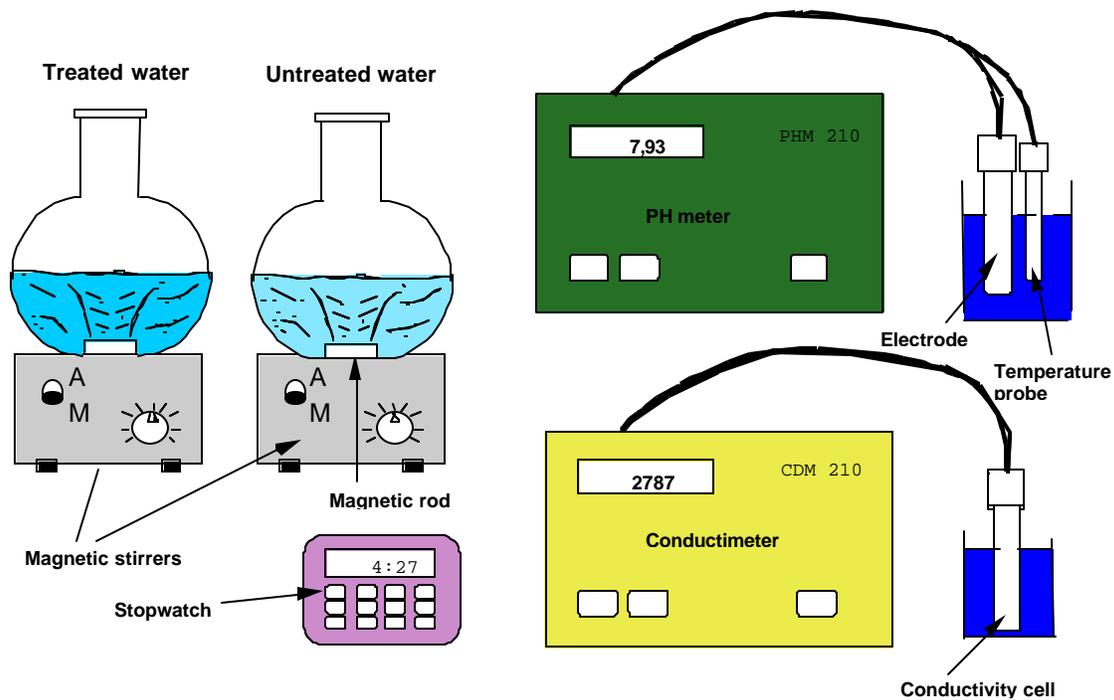

Fig. 13. RCP experimental device [Lédion et al., 1998].

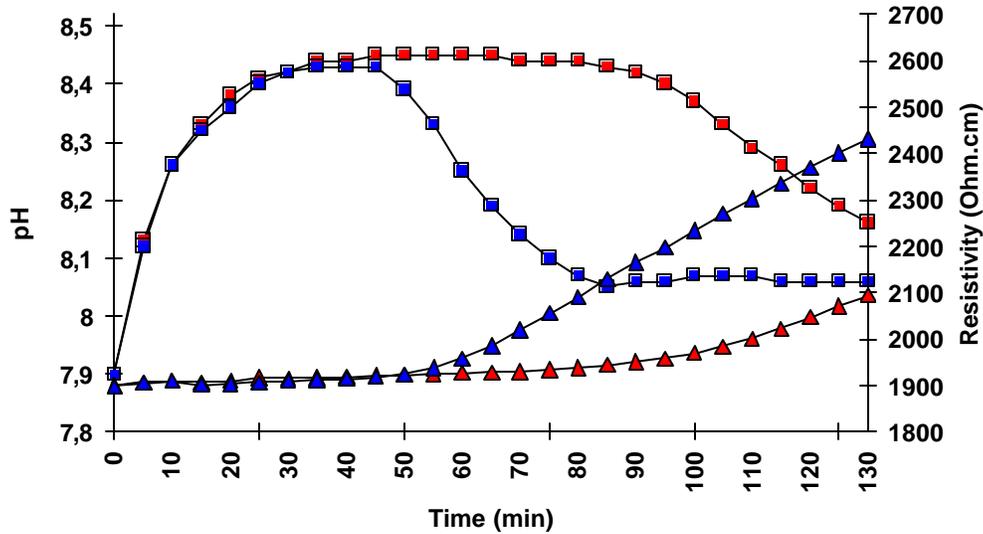*Montage expérimental de la méthode de Précipitation Contrôlée Rapide*

Figure 14. Example of RCP test, variation of pH and resistivity versus time (Red: treated water; Blue: non treated water) *[Lédion et al., 1998].*

Exemple des courbes de la méthode PCR, variation du pH et de la résistivité en fonction du temps d'essai (rouge: eau traitée; bleu: eau non traitée)

Polymer scaling test

By using the same CO_2 degassing procedure, Lédion et al. also proposed a gravimetry method called "polymer scaling test" (Lédion et al., 1993). It is based on electrostatic trapping of $CaCO_3$ nuclei by an insulating polyethylene wall. The experimental set-up is described in Figure 15. The specimen is a polyethylene tube. It is immersed in an austenitic stainless steel beaker containing the test water which is degassed by magnetic stirring. Test and reference specimens are cleaned prior to use followed by weighing on a balance accurate to a tenth of a milligram. After testing, the specimens are removed from the beaker lids, dried and then stabilised for a sufficient long time in the balance room and weighed. The weight gain due to the deposit was determined, taking into account the weight variation of the reference specimen.

Lid

Water level (700ml)

Tubular polyethylene specimen (Immersed surface area=235cm²)

Stainless steel beaker

Magnetic rod

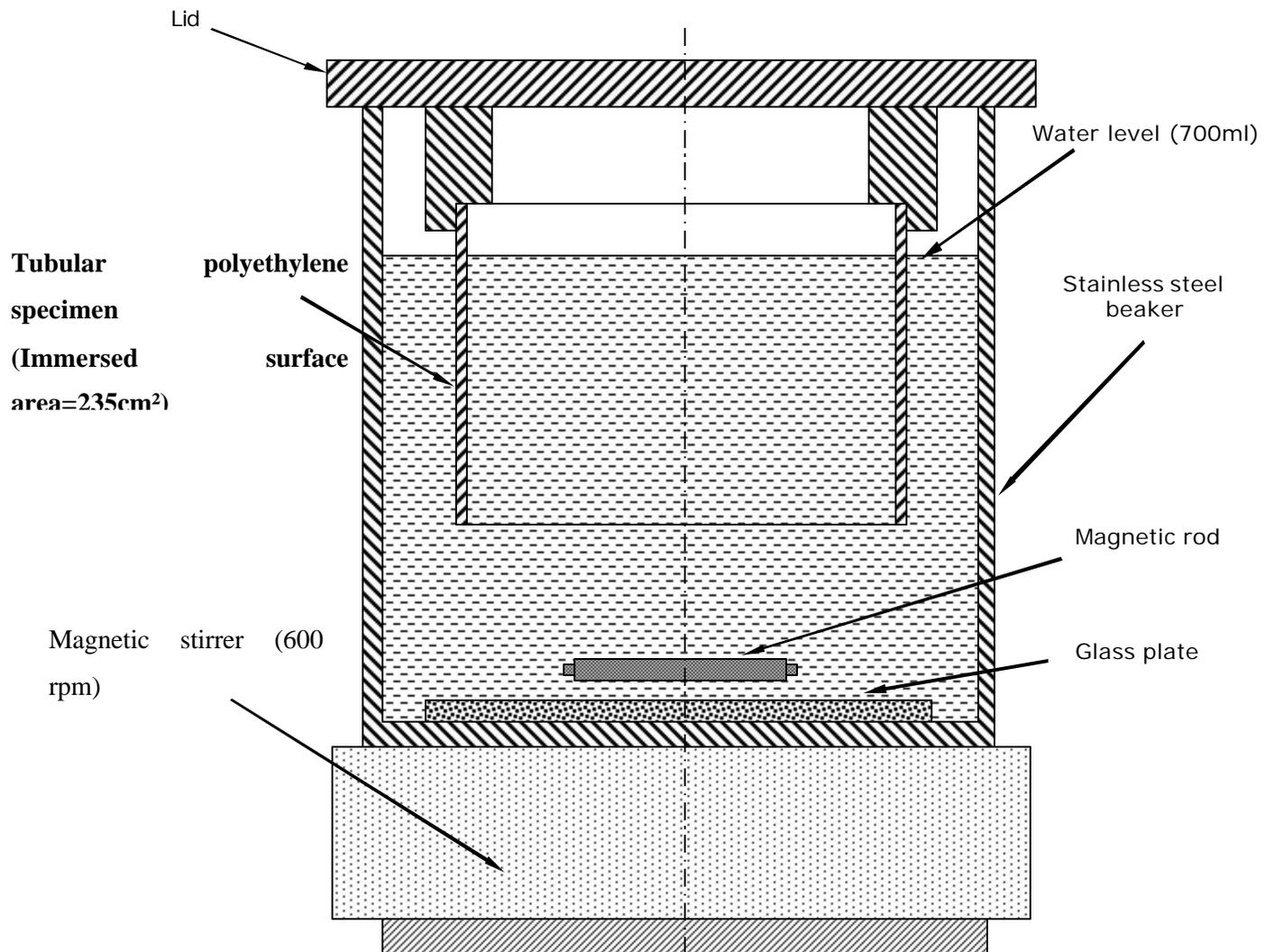Magnetic stirrer (600 rpm)

Glass plate

Figure 15 - Experimental set-up of polymer test [Lédion et al., 1993].

Montage expérimental du test sur polymères.

Continuous test

To simulate a real scaling procedure in hot water circuits, Lédion et al. (Lédion et al., to be published) have designed a test system called "continuous test rig" which is shown schematically in Fig. 16. The rig is designed so that the waters studied begin slightly to precipitate. This enables tests with a hot water circuit leading to scaling of the studied materials. The tubes are mounted in series with plastic joints and their positions are changed every day by circular permutation, to compensate for possible variations in copper ion concentration that could modify the scaling potential of the water at different points in the circuit. The temperature of the water was controlled by a thermostat bath at ±0.1, and the outlet flow rate was maintained at about 35 L/h. For each series of specimens, the tests lasted 30 days, with 8 hours exposure per day, i.e. a total of 240 hours. Scaling was evaluated by weighing on a balance accurate to a tenth of a milligram. To avoid unwanted scale nucleation due to water evaporation, the specimens were withdrawn after each exposure period, when the water had cooled to ambient temperature. They were then rinsed in demineralized water and oven dried for 20 minutes at 50°C. Weighing was performed after the tubes had cooled to the temperature of the balance room.
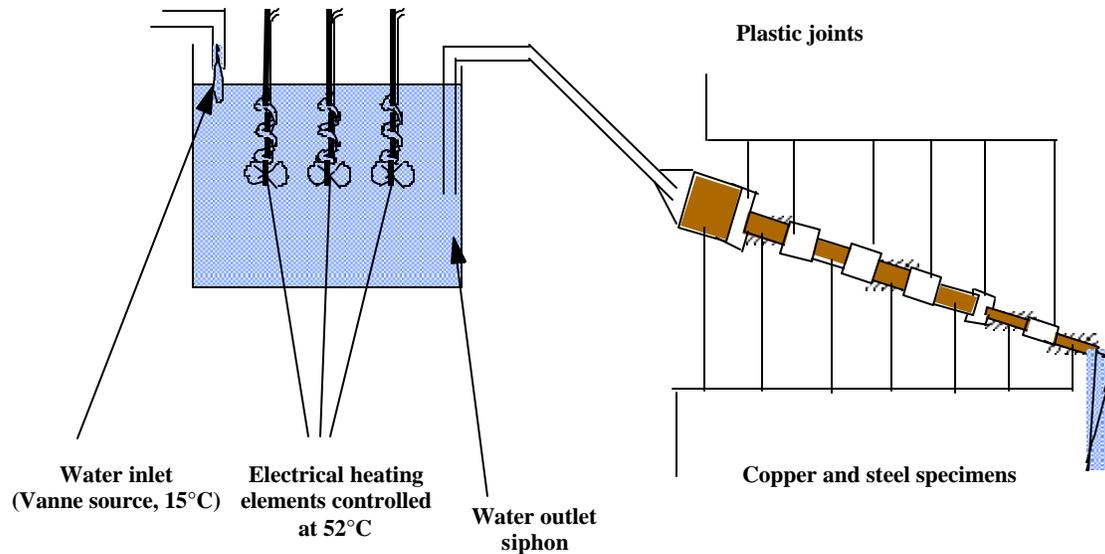
Figure 16. Principle of the continuous test rig [Lédion et al., to be published].

Principe du test en continu sur tubes.

DISCUSSION AND CONCLUSION

All these methods that are complementary one each other have contributed to improving our knowledge on $CaCO_3$ precipitation, scaling potential evaluation and scaling mechanisms.

Nevertheless, it is necessary to take into consideration their representativeness in relation to a real scaling phenomenon. After all, an accelerated test is not always an accurate representation of a real scaling formation which may develop over several months or even several years, and which brings into play not only the water's intrinsic characteristics but also complex water distribution installations and materials.

Therefore, at best the accelerated scaling methods only make it possible to characterise the water's scaling capacity. When looking at the different methods available, it is interesting to compare the conditions in which $CaCO_3$ precipitation or scaling has been obtained. However, before doing this, it is better to consider thermodynamic and kinetic aspects of $CaCO_3$ precipitation.

In fact, for the precipitation of solid calcium carbonate to effectively appear from a liquid phase, nuclei must be able to form and grow. The process starts with the formation of pairs of hydrated CO_3^{2-} and Ca^{2+} ions, which group together to create a colloidal nucleus possessing an electrical charge, characterised by its potential ζ. This nucleus grows and at the same time gradually loses its hydrate molecules, to finally form a crystal, which then has its own growth phase.

For nucleation to occur, the reaction $CO_3^{2-} + Ca^{2+} \rightarrow CaCO_3 \downarrow$ must be thermodynamically possible. This will be the case when the ionic concentrations exceed the solubility product. In particular, it depends on the temperature and the ionic force due to all the species present in the water. At any point in a water circuit, the local conditions can be defined by

$$[Ca^{2+}] . [CO_3^{2-}] = \delta\, K'_s$$

where K'_s is the solubility product.

When $\delta < 1$ the water is locally *aggressive.*

When $\delta = 1$ the water is locally *in thermodynamic equilibrium.*

When $\delta > 1$ the water is *calcifying* and calcium carbonate is thermodynamically liable to precipitate. The value of δ can be easily calculated by the Legrand-Poirier method [6]. However, both thermodynamic considerations and experience show that it is not sufficient for δ to be just greater than 1 for detectable nucleation to occur. For massive irreversible nucleation leading to precipitation, δ must attain a value of the order of 40 [Tarits 1990]. Above this value, precipitation in the water is virtually certain. For values between 1 and 40, precipitation remains possible, with an increasing probability as δ approaches 40. In other words, when $\delta > 40$, the water which is completely unstable is characterised by spontaneous precipitation; if $1 < \delta < 40$ the water which is simply metastable is brought to the oversaturation level of real scaling phenomenon.

However, it has been shown (Deslouis et al., 1996) that in the electrochemical methods the water samples studied reached a d saturation level much higher than 40 in proximity of the electrode. The calculation by Legrand-Poirier method demonstrates that the same order of d values are obtained for other methods described above except for the RCP and the Polymer scaling tests. That is, an oversaturation degree lower than 40 is only reached by a moderated CO_2 degassing process. In fact, by using a stirring speed of 800 rpm, a d value of 25 is obtained at 23 °C for RCP (Lédion et al., 1998). Therefore, the RCP and the Polymer scaling test are more representative to a real scaling phenomenon than other methods.

REFERENCES

Deslouis C., I. Frateur, G. Maurin, B. Tribollet. 1996. Procédé de mesure in situ du pH interfacial au cours d'une réaction électrochimique. Application à l'étude de la réduction de l'oxygène dissous, dans une cellule à jet immergé. JIE96, Poitiers.

Deslouis C., C. Gabrielli, M. Keddam, , A. Khalil, R. Rosset, B. Tribollet, M. Zidoune. 1997. Impedance techniques at partially blocked electrodes by scale deposition. Electrochem. Acta 42(8) : 1219-1233.

Duffau C., J. P. Turchet, A. Sandra. 1995. Etude thermochimique de l'entartrage à l'aide du Scalmatic-batch. L'Eau, l'Industrie, les Nuisances 186: 50-55.

Elfil H., H. Roques. 2001. Role of hydrate phases of calcium carbonate on the scaling phenomenon. Desalination, 137 : 177-186.

Euvrard M., J. Lédion, Ph. Leroy. 1997. Effects and consequences of electric treatment in preventing scaling in drinking water systems. J. Water SRT-Aqua 46: 71-83.

Feitler H. 1972. The scale meter: a new method for determining the critical pH of scaling. Mater. Prot. Proform. **11** (1) : 31-35.

Gabrielli C., M. Keddam, H. Perrot , A. Khalil, R. Rosset, M. Zidoune, 1996a. Characterization of the efficiency of antiscale treatments of water – Part I : Chemical processes. J. Appl. Electrochem. 26: 1125-1132.

Gabrielli C., M., Keddam, G. Maurin, H. Perrot, R. Rosset, M. Zidoune. 1996b. Estimation of the deposition rate of thermal calcareous scaling by the electrochemical impedance technique. J. Electroanal. Chem. 412: 189-193.

Gabrielli C., M. Keddam, A. Khalil, R. Rosset, M. Zidoune. 1997. Study of calcium carbonate scales by electrochemical impedance spectroscopy. Electrochim. Acta. 42(8) : 1207-1218.

Gabrielli C., M. Keddam, A. Khalil, G. Maurin, H., Perrot, R. Rosset, M. Zidoune, 1998. Quartz crystal microbalance investigation of electrochemical calcium carbonate scaling. J. Electrochem. Soc. 145(7): 2386-2396.

Gabrielli C., G. Maurin, G. Poindessous, R. Rosset. 1999. Nucleation and growth of calcium carbonate by an electrochemical scaling process. J. Crystal Growth 200 : 236-250.

Gal J.Y., Y. Fovet, N. Gache. 1999. About scaling power evaluation of some mineral waters. European J. water Quality 30 (2): 179-199.

Hort C. 1994 Contribution à l'étude des phénomènes d'entartrage: Influence des solides en contact avec le liquide sur la cinétique de précipitation. Dissertation Thesis, INSA de Toulouse, France.

Khalil A., P. Sassiat, C. Colin, C. Meignen, C. Garnier, C. Gabrielli, M. Keddam, R. Rosset. 1992. Water scaling tendency characterization by coupling constant potential chronoamperometry with quartz crystal microbalance. C. R. Acad. Sci. Paris 314 (2): 145-149.

Lédion, J., P. Leroy, J.P. Labbé. 1985. Détermination du caractère incrustant d'une eau par essai d'entartrage accéléré. TSM – L'eau 80(7-8) : 323-328.

Lédion J., Y. Gueugnon, C. Ribal, P. Combaz, J. Verdu. 1993. L'entartrage des Matières Plastiques. TSM l'Eau 7-8 : 355-360.

Lédion J., B. François, J. Vienne. 1998. Caractérisation du pouvoir entartrant de l'eau par Précipitation Contrôlée Rapide. Journal Européen d'Hydrologie 28 (1) : 15-35.

Lédion J., C. Braham, F. Hui. The scaling behaviour of copper. J. Water SRT-Aqua, to be published.

Legrand L., G. Poirier, P. Leroy. 1981. Les équilibres carboniques et l'équilibre calcocarbonique. Eyrolles, Paris.

Legrand L. and P. Leroy. 1990. Prevention of corrosion and scaling in water supply systems. Ellis Horwood series in water and waste technology, N.Y.

Lin W., C. Colin, R. Rosset. 1990. Caractérisation du pouvoir incrustant d'une eau par chronoampérométrie au potentiel optimal d'entartrage. TSM – L'eau 12 : 613-620.

Lin W. and P. Combaz, 1995. Hebert, C. & Perichon C. Détection automatique de la menace d'entartrage du circuit de refroidissement d'une centrale nucléaire. L'Eau, l'Industrie, les Nuisances : 180, 51-54.

Leroy P., W. Lin, J. Lédion, A. Khalil. 1993. Caractérisation du pouvoir entartrante des eaux à l'aide d'essai d'électrodéposition – étude comparative de plusieurs méthodes. J. Water SRT-Aqua 42 (1): 23-29.

Roques, H. 1990. Fondements théoriques du traitement chimique des eaux. Tec & Doc, Lavoisier, Paris.

Rosset, R. 1992 Les procédés physiques antitartre: mythe ou réalité? L'actualité chimique 1-2 : 125-148.

Rosset R. 1993. Les méthodologies d'études des procédés antitartre. TSM – L'eau 11: 563-569.

Rosset R., M. Zidoune, C. Gabrielli, M. Keddam, G. Maurin, H. Perrot. 1996. Caractérisation du pouvoir entartrant d'une eau et évaluation de l'efficacité d'un traitement antitartre chimique au moyen d'une sonde thermique. C. R. Acad. Sci. Paris 322 (2b) : 335-341.

Rosset. R., D. Mercier, S. Douville. 1997. La mesure du pouvoir entartrant des eaux par des méthodes électrochimiques et les procédés antitartre. Ann. Fals. Exp. Chim.938 : 41-56.